Chemistry–A European Journal
Research Article
doi.org/10.1002/chem.202203317
Chemistry Europe
European Chemical Societies Publishing
www.chemeurj.org

$[ReH_3(PPh_3)_4]$ – A Key Compound in the Rhenium Hydride Chemistry

Maximilian Roca Jungfer*[a, b] and Ulrich Abram[a]

Abstract: The chemistry of the rhenium trihydrido complex $[ReH_3(PPh_3)_4]$ (**1**) has been reinvestigated. An improved synthesis and the solid-state structure of the compound as well as several reactions are reported. The solid-state structure of **1** is similar to that of $[TcH_3(PPh_3)_4]$ having a capped-octahedral coordination sphere. The PPh_3 ligands surround the Re atom in a trigonal-pyramidal mode with a short apical Re–P bond (2.300(2) Å) and three longer basal bonds (2.429(2)–2.449(2) Å). Reactions of **1** with monodentate phosphines such as PMe_3 or PBu_3 give the mono-substituted complexes $[ReH_3(PPh_3)_3(PMe_3)]$ (**2**) and $[ReH_3(PPh_3)_3(PBu_3)]$ (**3**) under retention of the apical PPh_3 ligand and substitution of one of the basal PPh_3 ligands. The stability of the phosphine trihydride complexes decreases in the order $PPh_3 > PMe_3 > PBu_3$. Treatment of $[ReH_3(PPh_3)_4]$ with trityl hexafluorophosphate in CH_3CN does not result in a hydride abstraction, but gives the tetrahydrido cation $[ReH_4(NCCH_3)(PPh_3)_3]^+$ (**4**), while reactions with nitriles give unstable azavinylidene complexes of the composition $[ReH_2(PPh_3)_3(NC(H)R)]$ (**5**). They are formed by an insertion of the nitrile into a Re–H bond. The solid-state structure of the methyl derivative $[ReH_2(PPh_3)_3(NC(H)CH_3)]$ (**5a**) was determined showing a linear Re–N–C unit with rhenium–nitrogen and nitrogen–carbon double bonds, while the N=CH–C bond is clearly bent with an angle of 124°. Two previously unknown polymorphs of $[ReH_5(PPh_3)_3]$ were isolated from reactions of **1** with $HOC_6H_3(CH_3)_2$ and thiourea after prolonged heating in toluene and characterized by IR spectroscopy and X-ray diffraction.

Introduction

Rhenium polyhydrido complexes have constantly been studied since their initial discovery due to their interesting molecular properties such as structural fluxionality as well as high diversity in geometries and oxidation states, which have recently also been exploited in catalysis.[1–26] The most common synthetic protocols for the generation of rhenium polyhydrido compounds involve reactions of precursors containing suitable, stabilizing co-ligands such as phosphines or nitrogen donors. Such compounds react with complex hydrides like $LiAlH_4$ or $NaBH_4$ under formation of the desired hydrido rhenium complexes. Alternatively, rhenium polyhydrido complexes are often accessible through H_2-replacement from higher polyhydrides or by H_2-addition to lower (poly)hydrides of rhenium.[1–27] Mono-, di-, tri-, tetra-, penta-, hexa-, hepta-, octa- and enneahydrido complexes of rhenium are known. Thermodynamic and kinetic data describing hydride transfer reactions (the hydricity) in such systems are crucial parameters for the development of new and/or more active hydride catalysts.[28]

Some of the general procedures include the replacement of H_2 by organic ligands yielding $[ReH_{x-2}(L)_{8-x}L']$ from $[ReH_x(L)_{9-x}]$ complexes (L = phosphines and L′ = incoming ligands: phosphines, arsines, nitrogen donors such as nitriles or aromatic imines, alkenes, isonitriles and others),[17–19,26–30] ligand substitutions by H_2 in $[ReH_x(L)_{8-x}L']$ (L′ = leaving ligand) complexes to give $[ReH_{x+2}(L)_{8-x}]$,[26] hydride abstraction from $[ReH_x(L)_{9-x}]$ with $[CPh_3]^+$ to give $[ReH_{x-1}(L)_{9-x}]^+$,[17–19] protonation of $[ReH_x(L)_{9-x}]$ compounds with protic acids such as HBF_4 to give $[ReH_{x+1}(L)_{9-x}]^+$,[17–19] but also the deprotonation of $[ReH_x(L)_{9-x}]^+$ cations with bases such as NEt_3 under formation of $[ReH_{x-1}(L)_{9-x}]$ complexes has been observed.[17–19] A summary of typical interconversions involving various oxidation states of rhenium is shown in the Supporting Information, while parts of the interconversion involving trihydridorhenium(III) complexes is given in Scheme 1.

One of the key compounds of the hydrido chemistry of rhenium is $[ReH_3(PPh_3)_4]$ (**1**), the existence of which has already been mentioned in one of the very first pioneering works of Freni and co-workers.[25] Compound **1** plays a role in several interconversions between hydrido and dihydrogen complexes (see Scheme 1). These studies date back to the 1960's and laid the foundation for all subsequent studies about rhenium polyhydrides containing phosphine co-ligands.[10,25,27] Exemplarily, traces of the trihydride $[ReH_3(PPh_3)_4]$ were reported to be formed by the deprotonation of the tetrahydride cation $[ReH_4(PPh_3)_4]^+$ with NEt_3, although pure samples could not be isolated.[15] The tetrahydride cation $[ReH_4(PPh_3)_4]^+$ itself, however, was prepared by hydride abstraction from the pentahy-

[a] Dr. M. Roca Jungfer, Prof. Dr. U. Abram
Institute of Chemistry and Biochemistry
Freie Universität Berlin
Fabeckstr. 34/36, 14195 Berlin (Germany)
[b] Dr. M. Roca Jungfer
University of Heidelberg
Im Neuenheimer Feld 584, 69120 Heidelberg (Germany)
E-mail: mrj666@hotmail.de
maximilian.roca.jungfer@uni-heidelberg.de

Supporting information for this article is available on the WWW under https://doi.org/10.1002/chem.202203317

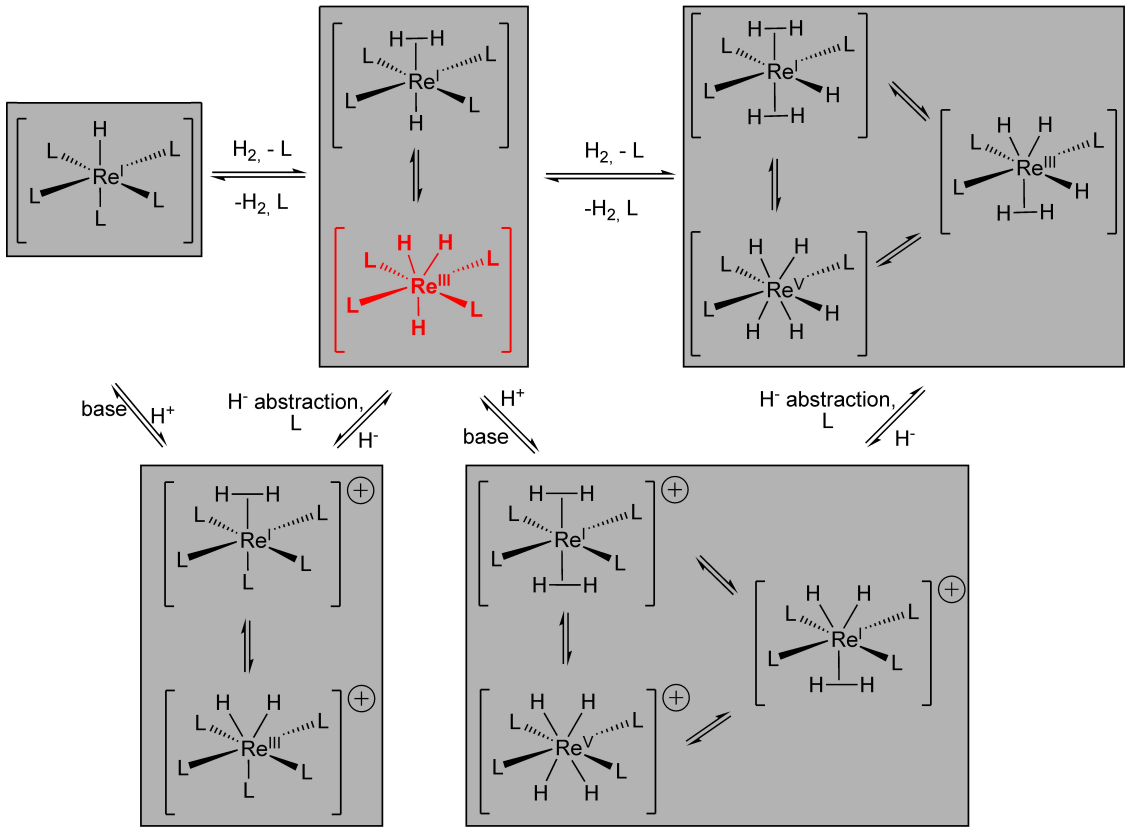

Scheme 1. Hydridorhenium(III) complexes and their interconversion to other hydrido species.[17–19,26–30]

dride $[ReH_5(PPh_3)_3]$.[15] In this context, it was surprising to note that $[ReH_3(PPh_3)_4]$ itself is only scarcely described and no reliable synthesis or detailed spectroscopic and structural data have been reported up to now.

In a recent paper, we extensively studied the hydrido chemistry of low-valent technetium complexes with $[TcH_3(PPh_3)_4]$ as one of the key-compounds.[31] It turned out that this complex can be synthesized in reasonable amounts and high purity and possesses a versatile ligand exchange chemistry. The obtained results stimulated us to also reinvestigate the synthesis, properties, and reactivity of its rhenium analogue: $[ReH_3(PPh_3)_4]$ (**1**).

Results and Discussion

Synthesis and properties of $[ReH_3(PPh_3)_4]$ (1)

The first synthesis of $[ReH_3(PPh_3)_4]$ was reported in the 1960's by Freni and Valenti.[25] The compound was described as a brick-red product isolated from a reaction between '$Re^{II}I_2(PPh_3)_2$' and $NaBH_4$. The existence of stable four-coordinate rhenium(II) complexes was widely accepted that time and also '$ReCl_2(PPh_3)_2$',[32,33] which was later shown to be the nitrido complex $[Re^{V}NCl_2(PPh_3)_2]$,[34,35] was frequently used as a common starting material. Thus, we assume, that the starting material used by Freni for the synthesis of $[ReH_3(PPh_3)_4]$ was actually $[Re^{IV}OI_2(PPh_3)_2]$, which is formed under the conditions described.[36]

Based on our recent advances in the preparation of benchstable $[TcH_3(PPh_3)_4]$ and the fact that most probably also the classic synthesis of **1** started from a Re(IV) compound, we used the readily accessible $[ReCl_4(PPh_3)_2]$ as starting material for our experiments (Scheme 2). The sparingly soluble red compound was treated with $NaBH_4$ in a hot mixture of toluene and ethanol, which resulted in an immediate H_2 evolution and a color change to orange-yellow. After hydrolysis of the residual borohydride, the product could be isolated as air-stable yellow microcrystals.

The ν_{Re-H} vibration in the IR spectrum of $[ReH_3(PPh_3)_4]$ is detected at 1973 cm^{-1}. This value corresponds to a blue-shift of about 80 cm^{-1} compared to that obtained for $[TcH_3(PPh_3)_4]$ indicating that the hydrido ligands in the rhenium compound are bound more tightly. For comparison, the known protonated $[ReH_4(PPh_3)_4]^+$ cation shows the IR stretch in the same region at

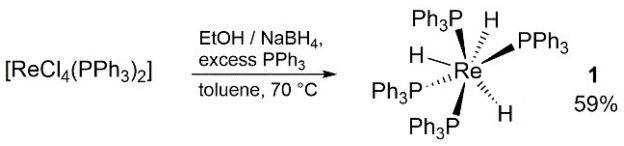

Scheme 2. Synthesis of $[ReH_3(PPh_3)_4]$ (**1**).

2020 cm^{-1}.[10] The more narrow ν_{Re-D} band of partially deuterated $[ReH_3(PPh_3)_4]$ is found at 1715 cm^{-1}. Surprisingly, the ESI+ mass spectrum of $[ReH_3(PPh_3)_4]$ shows major signals only for $[ReH(PPh_3)_3]^+$ and $[ReH_3(PPh_3)_4]^+$, while the formation of $[ReH_4(PPh_3)_4]^+$ is not observed. This is unusual given the feasibility of the protonation of rhenium trihydrides to give rhenium tetrahydrides. It is, however, consistent with the observed inability to protonate the $[MH_3(PPh_3)_4]$ (M = Tc, Re) complexes to give the corresponding $[MH_4(PPh_3)_4]^+$ species in our hands. In contrast, the cationic tetrahydride $[ReH_4(PPh_3)_4]^+$ was readily prepared via a protonation/H_2-elimination route from $[ReH_5(PPh_3)_3]$ in the presence of excess PPh_3.[10]

In the ^{1}H NMR spectrum, the hydride resonance of $[ReH_3(PPh_3)_4]$ is observed as a quintet at −7.54 ppm with a $^2J_{P-H}$ of 40.4 Hz in benzene-d_6. Thus, the resonance is shifted up-field compared to that of the technetium analogue, while the $^2J_{P-H}$ coupling is slightly increased. In comparison to $[ReH_4(PPh_3)_4]^+$ [$\delta(^1H)$ = −2.60 ppm; $^2J_{P-H}$ = 25.6 Hz], both the up-field shift and the increase of $^2J_{P-H}$ are considerably larger.[10,37] A similar trend is found when the ^{1}H NMR spectrum of $[ReH_3(PPh_3)_4]$ is compared with those of other phosphine-substituted rhenium trihydrido complexes such as $[ReH_3(PPh_2Me)_4]$ [$\delta(^1H)$ = −6.1 ppm; quint; $^2J_{P-H}$ = 20 Hz] and $[ReH_3(PPhMe_2)_4]$ [$\delta(^1H)$ = −6.80 ppm; quint; $^2J_{P-H}$ = 20 Hz].[6,12] The related phosphonite complexes $[ReH_3\{P(OEt)_2Ph\}_4]$ and $[ReH_3\{PPh_2(OEt)\}_4]$ show chemical shifts of −5.2 (quint, $^2J_{P-H}$ = 18 Hz) and −6.6 ppm (quint, $^2J_{P-H}$ = 18 Hz).[8] Other structurally related complexes are $[ReH_3(PPh_3)_2(dppe)_2]$ [$\delta(^1H)$ = −6.27 ppm; s; $^2J_{P-H}$ = 10 Hz; $\delta(^1H)$ = −6.75 ppm; quint; $^2J_{P-H}$ = 24 Hz], $[ReH_3(dppe)_2]$ [$\delta(^1H)$ = −7.97 ppm; quint; $^2J_{P-H}$ = 17 Hz], $[ReH_3(PPh_3)_2\{P(OPh)_3\}_2]$ [$\delta(^1H)$ = −6.1 ppm; quint; $^2J_{P-H}$ = 21.4 Hz], $[ReH_3(PPh_3)\{P(OPh)_3\}_3]$ [$\delta(^1H)$ = −7.2 ppm; quint; $^2J_{P-H}$ = 18 Hz], $[ReH_3(CH_3CN)(PPh_3)_3]$ [$\delta(^1H)$ = −6.27 ppm; q; $^2J_{P-H}$ = 15.7 Hz] and $[ReH_3(CNBu^t)(PPh_3)_3]$ [$\delta(^1H)$ = −5.00 ppm; q; $^2J_{P-H}$ = 22.0 Hz]. The hydrido ligands in all these complexes exhibit only half of the observed coupling constant found for $[ReH_3(PPh_3)_4]$, but resonate in a similar chemical shift range.[6,18,24] The estimation of the minimum ^{1}H T_1 relaxation time for the hydrido ligands is sometimes used as a discriminator for the dihydride vs. dihydrogen coordination modes in polyhydride complexes.[15,16,20,37] This parameter, however, is not always a valid criterion, especially in the case of rhenium polyhydrido complexes as has exemplarily been described for the related compounds $[ReH_3(PPhMe_2)_4]$ and $[ReH_3(PPh_2Me)_4]$.[12,13] The T_1(min) values of these trihydrides are inconsistent with their assignment as classical hydrido complexes. The T_1 relaxation time of $[ReH_3(PPh_3)_4]$ was estimated by an inversion recovery experiment at room temperature. The exponentially fitted relaxation curve gives a t_0 value of 117 ms and the resulting T_1(RT) of 169 ± 12 ms indicates a similar situation as observed for the related trihydrides and, thus, the determination of a T_1(min) was omitted. But considering additionally that no H–H stretching frequencies are detected in the IR spectrum of **1**, we are confident to assign $[ReH_3(PPh_3)_4]$ as a classical hydrido complex as its technetium analog.[31] Other Re–D vibrations are given in the Supporting Information. DFT calculations on the B3LYP level support this claim and show that the bonding situation in $[ReH_3(PPh_3)_4]$ is similar to that in $[TcH_3(PPh_3)_4]$ and the hypothetical manganese analogue $[MnH_3(PPh_3)_4]$ (further information is given as Supporting Information).

Similarly to the technetium compound, $[ReH_3(PPh_3)_4]$ tends to form microcrystalline powders upon (re)crystallization. Thus, we adopted the successful strategy used for the crystallization of $[TcH_3(PPh_3)_4]$ for the growth of single crystals of **1**. Indeed, $[ReH_3(PPh_3)_4]$ readily crystallizes from a dilute reaction mixture upon storage in a freezer as large yellow-green crystals. Two polymorphs were identified: a hexagonal one (space group $P6_3/m$) with a four-fold disorder of the whole molecule over the space-group symmetry and a triclinic one (space group $P\bar{1}$). The triclinic form of **1** crystallizes as toluene solvate as the technetium analogue and shall be used for the following structural discussion. Details about the hexagonal polymorph are given as Supporting Information.

The solid-state structure reveals an isostructural arrangement of the heavy atoms compared to the analogous technetium compound.[30] The molecular structure of **1** is shown in Figure 1. Selected bond lengths and angles are compared to the values in the other trihydrido complexes of this study in Table 1. Three phosphorus donor atoms form the basis of a trigonal pyramid with similar Re–P bond lengths between 2.429(2) Å and 2.459(2) Å, while the bond to the apical phosphorus atoms P4 is significantly shorter (2.300(2) Å). This is due to the strong *trans*-influence of the opposing hydrido ligands of the three basal phosphine ligands. The same bonding pattern has been found for $[TcH_3(PPh_3)_4]$, where the positions of the three hydrido ligands could be derived from the final Fourier map and refined. Given the close similarity of the phosphine-arrangements in $[TcH_3(PPh_3)_4]$ and $[ReH_3(PPh_3)_4]$, we placed the hydrido ligands in **1** on chemically similar positions.

It is worth to compare the P–Re–P bond angles and Re–P bond lengths of this complex also with those found for the known $[ReH_4(PPh_3)_4]^+$ cation, which was prepared by the reaction of $[ReH_5(PPh_3)_3]$ and $[HPPh_3][BF_4]$.[10] In the tetrahydrido cation, all Re–P bond lengths are similar with values between 2.43 Å and 2.47 Å, while the hydride positions were not located.[10] The phosphines span a flattened tetrahedron with four *cis* bond angles of ca. 98° and two *trans* bond angles of ca.

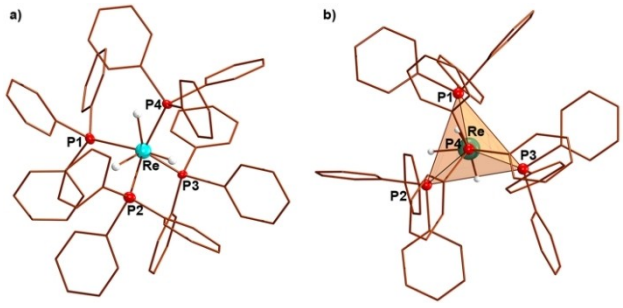

Figure 1. Molecular structure of $[ReH_3(PPh_3)_4]$ (**1**), a) wire representation with ball and stick model on Re-bound atoms (hydride positions were not located in the density map and adopted from the analogous technetium complex) and b) polyhedron around the rhenium atom. Further labels and hydrogen atoms bonded to carbon atoms are omitted for clarity.

Table 1. Selected bond lengths [Å] and angles [°] in the solid state structures of $[ReH_3(PPh_3)_4]$ (**1**), $[ReH_3(PPh_3)_3(PMe_3)]$ (**2**), $[ReH_3(PPh_3)_3(PBu_3)]$ (**3**) and $[ReH_2(NCHCH_3)(PPh_3)_3]$ (**4a**).

	$[ReH_3(PPh_3)_4]$ (**1**)	$[ReH_3(PPh_3)_3(PMe_3)]$ (**2**)	$[ReH_3(PPh_3)_3(PBu_3)]$ (**3**)	$[ReH_2(NCHCH_3)(PPh_3)_3]$ (**4a**)
P1–Re1	2.436(2)	2.4237(7)	2.452(2)	2.364(2)
P2–Re1	2.459(2)	2.4219(7)	2.428(2)	2.361(3)
P3–Re1	2.429(2)	2.4028(7)	2.420(2)	2.369(2)
P4(N1)–Re1	2.300(2)	2.2775(7)	2.291(2)	1.871(8)
C1–N1	–	–	–	1.29(1)
C1–C2	–	–	–	1.44(2)
P4(N1)–Re1–P3	109.90(6)	113.62(2)	120.37 (6)	87.9(2)
P4(N1)–Re1–P1	113.31(7)	116.86(2)	119.98 (5)	87.5(2)
P3–Re1–P1	108.64(6)	103.41(2)	98.09 (5)	162.80(9)
P4(N1)–Re1–P2	115.09(7)	123.47(2)	112.83 (5)	116.9(3)
P3–Re1–P2	105.34(6)	99.12(2)	100.44 (5)	97.27(9)
P1–Re1–P2	104.04(7)	96.98(2)	101.77 (5)	99.59(9)
N1–C1–C2	–	–	–	124(1)
C1–N1–Re1	–	–	–	178(1)

134°.[10] The similarity of the bond lengths in $[ReH_4(PPh_3)_4]^+$ to those of the three basal phosphorus atoms in $[ReH_3(PPh_3)_4]$ further support a *trans* occupation of the hydrido ligands as in $[TcH_3(PPh_3)_4]$. We believe that the main structural differences between $[ReH_3(PPh_3)_4]$ and $[ReH_4(PPh_3)_4]^+$ result from the additional hydrido ligand occupying the position *trans* to the apical phosphorus atom P4 in the trihydrido compound **1**. Thus, the Re–P bond lengths are equalized in the cationic compound, which finally results in the formation of a H,H,H,H tetrahedron intersecting a P,P,P,P flattened tetrahedron.

Even though solutions of $[ReH_3(PPh_3)_4]$ are more stable than those of its technetium analogue, they subsequently decompose with traces of water to the well soluble pentahydride $[ReH_5(PPh_3)_3]$ and release $OPPh_3$. The viability of $[ReH_3(PPh_3)_4]$ for the formation of $[ReH_5(PPh_3)_3]$ was already documented by Freni et al. and a thermal reaction between $[ReH_3(PPh_3)_4]$ with a large excess of $NaBH_4$ led to the initial discovery of the pentahydride $[ReH_5(PPh_3)_3]$.[26] Storing solutions of **1** for prolonged time or heating them without suitable ligands gives $[ReH_5(PPh_3)_3]$ and PPh_3 as the predominant decomposition products, while solid $[ReH_3(PPh_3)_4]$ is stable under inert conditions. All our attempts to avoid the decomposition of $[ReH_3(PPh_3)_4]$ under formation of $[ReH_5(PPh_3)_3]$ (alongside other side-products) in aromatic hydrocarbon or chlorinated solvent solutions were unsuccessful. It should be noted that related trihydridorhenium complexes with more basic or chelating phosphines as well as chelating nitrogen donors appear to be much more stable.[8,17,27] The observed high reactivity suggests $[ReH_3(PPh_3)_4]$ as a valuable starting material for ligand exchange reactions as has been demonstrated before for $[TcH_3(PPh_3)_4]$.[31]

Reactions of $[ReH_3(PPh_3)_4]$ with phosphines

Freni et al. observed that complexes of the type $[ReH_3(PR_3)_4]$ (R = alkyl, aryl, alkoxyl, alkoxaryl) react photochemically with other phosphines or phosphites under formation of di- or tri-substituted complexes and mixtures thereof. The mono- and tetra-substituted products with monodentate phosphines and phosphites, however, could not be isolated.[24,27,38] Similarly, $[TcH_3(PPh_3)_4]$ rapidly forms mixtures containing a variety of polysubstituted species when reacted with other monodentate ligands.[31] The mixed-phosphine complex $[TcH_3(PPh_3)_2(PMe_3)_2]$ could be isolated as a bright yellow microcrystalline substance from such a reaction, which motivated use to reinvestigated such reactions also with the rhenium complex **1** (Scheme 3).

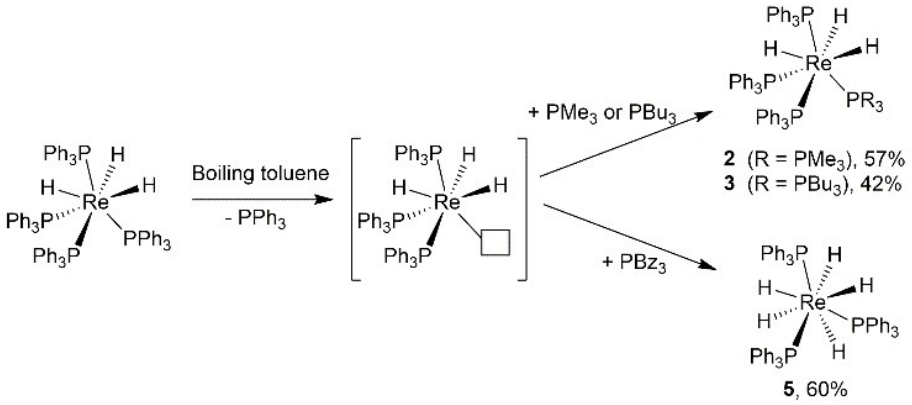

Scheme 3. Reactions of $[ReH_3(PPh_3)_4]$ (**1**) with monodentate phosphines.

Keeping in mind the slower kinetics in exchange reactions of rhenium compared to technetium,[39] there should be a good chance for the isolation of such mixed-phosphine species.

The rhenium analogue is indeed more inert. Reactions of $[ReH_3(PPh_3)_4]$ with phosphines require temperatures of approximately 70 °C. At this temperature, the priorly insoluble starting material dissolves instantaneously to give a blood-red solution. We assume, that the crucial step is the thermal release of a PPh_3 ligand from the starting complex at this temperature, which gives an intermediate 6-coordinate compound (Scheme 3). The immediate addition of methanol to the formed, clear reaction mixture results in the precipitation of bright yellow crystals of the mono-substituted complexes $[ReH_3(PPh_3)_3(PMe_3)]$ (**2**) and $[ReH_3(PPh_3)_3(PBu_3)]$ (**3**). The single substitution is readily verified by the doublet of quartets splitting pattern of the respective hydrido ^{1}H NMR resonances and the doublet splitting for the PPh_3 phosphorus atom resonance alongside the quartet splitting of the PR_3 (R = Me, Bu) phosphorus atom resonances with a 3:1 integral ratio in their $^{31}P\{^1H\}$ NMR spectra. The observation of single resonances indicates that the structures of the products are fluxional at room temperature and equalize the PPh_3 phosphorus nuclei as well as the hydrido ligands.

Prolonged reaction times lead to intractable reaction mixtures containing well-soluble, but unstable, multiply substituted products alongside decomposition products such as pentahydrido complexes as was observed before.[24,27,38] The colorless pentahydrido complex $[ReH_5(PPh_3)_3]$ is also formed instead of the intended phosphine substitution product when tris(benzyl)phosphine, $P(Bz)_3$, is used. Such a behavior can be attributed to the presence of potentially abstractable benzylic β-hydrogen atoms (Scheme 3).

The $[ReH_3(PPh_3)_3(PR_3)]$ (R = Me, Bu) complexes are highly soluble in common nonpolar solvents such as toluene. The sterically more crowded monosubstituted complex of PBu_3 is less stable than the PMe_3 derivative. An obvious indication for the decomposition of the products is the slowly evolving smell of the alkyl phosphine released from the complexes even in the solid, crystalline state accompanied by the slow formation of brown oils.

Complex **3** is also unstable in solution and gradually decomposes into mixtures of $[ReH_5(PPh_3)_2(PBu_3)]$, $[ReH_5(PPh_3)_3]$, $[ReH_3(PPh_3)_4]$, $[ReH_3(PPh_3)_3(PBu_3)]$, PPh_3 and $OPBu_3$. Traces of these compounds are also visible in the ^{1}H and $^{31}P\{^1H\}$ NMR spectra of freshly prepared solutions. The ESI^+ mass spectrum of $[ReH_3(PPh_3)_3(PBu_3)]$ is similar to that of $[ReH_3(PPh_3)_4]$ and shows an intense signal of the fragment $[ReH(PPh_3)_2(PBu_3)]^+$ besides the molecular ion peak $[ReH_3(PPh_3)_3(PBu_3)]^+$. Since the coordination spheres of $[ReH_3(PPh_3)_3(PBu_3)]$ (**3**) as well as $[ReH_3(PPh_3)_4]$ (**1**) are crowded by rather bulky phosphine ligands, we assume steric repulsion as a driving force for the decomposition via unsaturated fragments. In contrast, the PMe_3 derivative $[ReH_3(PPh_3)_3(PMe_3)]$ (**2**) is much more stable and only slowly releases traces of PPh_3. In contrast to those of **1** and **3**, the ESI^+ mass spectrum of $[ReH_3(PPh_3)_3(PMe_3)]$ (**2**) does not show a peak-group corresponding to the unsaturated $[ReH(PPh_3)_2(PMe_3)]^+$ fragment or the molecular ion peak. Instead, a peak-group for the protonated tetrahydrido cation $[ReH_4(PPh_3)_3(PMe_3)]^+$ is observed.

The formation of the tetrahydrido cation $[ReH_4(PPh_3)_3(PMe_3)]^+$ from **2** was unequivocally confirmed by the addition of aqueous HBF_4 to acetone solutions of **2**, which resulted in the formation of colorless crystals of $[ReH_4(PPh_3)_3(PMe_3)][BF_4]$·acetone. The crystals were of limited quality and details about the related X-ray diffraction study are given as Supporting Information. The determined structure is consistent with the detection of a novel singlet ^{1}H NMR resonance in the hydrido region at −3.33 ppm (FWHM (RT) = 23.7 Hz) in CD_2Cl_2. The mass spectrum of the product shows the same features as compound **2**.

Single crystals of the PMe_3 and PBu_3 derivatives **2** and **3** were grown by slow diffusion of methanol into dilute reaction mixtures in a refrigerator. In the case of the PBu_3 derivative, the positions of hydrido ligands could be derived from the Fourier maps and refined freely. For the PMe_3 derivative, the hydrido ligand positions were taken from the difference map and not refined. Figure 2 shows the molecular structure of the PMe_3 complex (**2**) together with the established, distorted P,P,P,P tetrahedron. Selected bond lengths and angles are summarized in Table 1. Structural details of $[ReH_3(PPh_3)_3(PBu_3)]$ can be found as Supporting Information.

Like in $[ReH_3(PPh_3)_4]$ (**1**), in the compounds **2** and **3** a distorted tetrahedral (trigonal pyramidal) arrangement of the four phosphine ligands with a base of three phosphine ligands, each with a hydrido ligand in *trans* position, and an apex of a fourth (more tightly bound) PPh_3 ligand is present. Interestingly, the hydrido ligands are here arranged *trans* to two PPh_3 ligands and one PR_3 ligand, which suggests that the strongly bound apical PPh_3 of **1** was not exchanged. The lability of the basal PPh_3 ligands can be attributed to the *trans* influence of the hydrido ligands and a resulting *trans* effect in this substitution reaction.

Generally, the substitution with the more basic alkyl phosphines contracts the averaged basal Re–P bond length from 2.441 Å in the starting material to 2.433 Å in the PBu_3 complex and 2.416 Å in the PMe_3 complex. The apical Re–P bond length decreases similarly and, thus, a substitution with

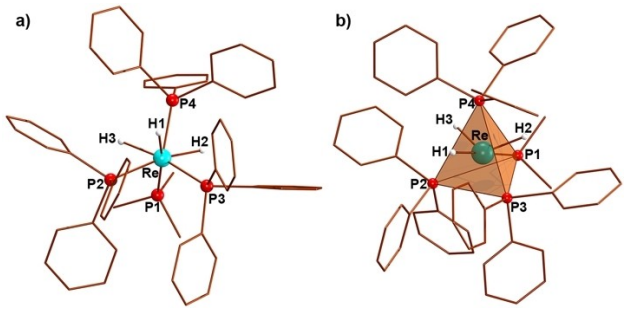

Figure 2. a) Wire representation with ball and stick model on Re-bound atoms in $[ReH_3(PPh_3)_3(PMe_3)]$ (**2**) and b) polyhedron around Re. The hydrido ligand positions were taken from the density map but were not refined. Further labels and hydrogen atoms bonded to carbon atoms are omitted for clarity.

alkyl phosphines appears to strengthen the Re–P bonds significantly. The Re–H bond lengths are generally in the range found for other rhenium polyhydrido complexes[10,31,40,41] but not discussed in detail due to their elusive nature.

At the first glance, the coordination geometry of **2** and **3** can be described as a distorted capped octahedron (7-COC) as its parent compound $[ReH_3(PPh_3)_4]$ (**1**). However, applying the SHAPE algorithm,[42–46] more favorable geometry factors can be derived for a capped trigonal prismatic geometry (7-CTPR) for both compounds. The differences mainly result from deviations in the *trans* P–Re–H bond angles, which lie between 168° and 171° (complex **3**) or 166° and 171° (complex **2**). The H–H contacts are between 2.4 Å and 2.8 Å for compound **3** and 2.6 Å and 3.1 Å for compound **2**. They are consistent with the assignment of both compounds as classical hydrido complexes and, thus, with the information derived from the room temperature ^{1}H NMR relaxation parameters of their respective hydrido resonances (see Supporting Information for details).

To better understand the differences in group 7 trihydrido tetrakisphosphine complexes, we performed DFT calculations on the related series of $[MH_3(PPh_3)_{4-x}(PMe_3)_x]$ (M = Mn, Tc, Re and x = 0, 1, 2, 3, 4) complexes. A detailed discussion of the respective structural changes is contained in the Supporting Information. In conclusion, this theoretical study indicates that all trihydrido complexes of the group 7 elements favor the formation of "elongated H_2-type" structures showing a rather pentagonal bipyramidal geometry with increasingly basic, sterically less-demanding phosphine donor ligands over the capped octahedral (or capped trigonal prismatic) arrangements. Although the "elongated H_2-type" complexes are disfavored along the group from manganese to rhenium, the dihydrogen character of the H_2-moiety in the pentagonal bipyramidal ligand arrangement increases inversely in the group from rhenium to manganese. The results are summarized in Scheme 4. The energetically less favored arrangements are shown in grey. But it should be mentioned that the energetic differences are subtle and fluxionality between the structures can be concluded.

The structural differences of the complexes result in characteristic shapes of the resultant simulated IR spectra, which agree with the so-far experimentally accessible derivatives $[ReH_3(PPh_3)_4]$, $[TcH_3(PPh_3)_4]$, $[ReH_3(PPh_3)_3(PMe_3)]$ and $[TcH_3(PPh_3)_2(PMe_3)_2]$.

Reactions of $[ReH_3(PPh_3)_4]$ with nitriles

The formation of $[ReH_3(PPh_3)_3(L)]$ complexes has been reported for a variety of ligands as the result of reactions of $[ReH_5(PPh_3)_3]$ with monodentate ligands such as nitriles or isonitriles.[18] They proceed by a hydride abstraction, followed by deprotonation of the intermediate $[ReH_4(PPh_3)_3(L)]^+$ salts. We envisioned a more direct approach using $[ReH_3(PPh_3)_4]$ as starting material. However, we mainly obtained complex mixtures, which seldomly allowed for the isolation of defined species. Exemplarily, reactions of $[ReH_3(PPh_3)_4]$ in neat acetonitrile led to the formation of red-brown intractable mixtures. This was also true for reactions with neat or dilute isocyanides such as CyNC and ^{t}BuNC. The observations are not entirely surprising as the formation of non-hydride rhenium(I) cations of the type $[Re(CNR)_4(PR_3)_2]^+$ was already reported for reactions of isonitriles with $[ReH_7(PR_3)_2]$ alongside the recovery of unreacted starting material, while no traces of $[ReH_3(L)_x(PR_3)_{4-x}]$ complexes were observed.[47] Also from reactions of $[ReH_7(PPh_3)_2]$, $[ReH_5(PPh_3)_2L]$ and $[ReH_4I(PPh_3)_3]$ defined mono hydride rhenium(III) complexes $[ReH(L)_4(PPh_3)_2]^{2+}$ could only be isolated in the presence of HBF_4.[19]

Contrarily, reactions of $[ReH_3(PPh_3)_4]$ with only a small excess of nitriles (acetonitrile, isopropylnitrile, benzonitrile) in benzene yield orange-red solutions. For acetonitrile, an orange-yellow powder consisting mainly of a mixture of $[ReH_3(NCCH_3)(PPh_3)_3]$ and $[ReH_5(PPh_3)_3]$ could be isolated from such a solution through the addition of methanol. When the methanol-containing reaction mixture is crystallized slowly in the cold, large deep red-brown crystals are slowly formed besides the yellow-orange powder. Due to the size of the crystals, they are

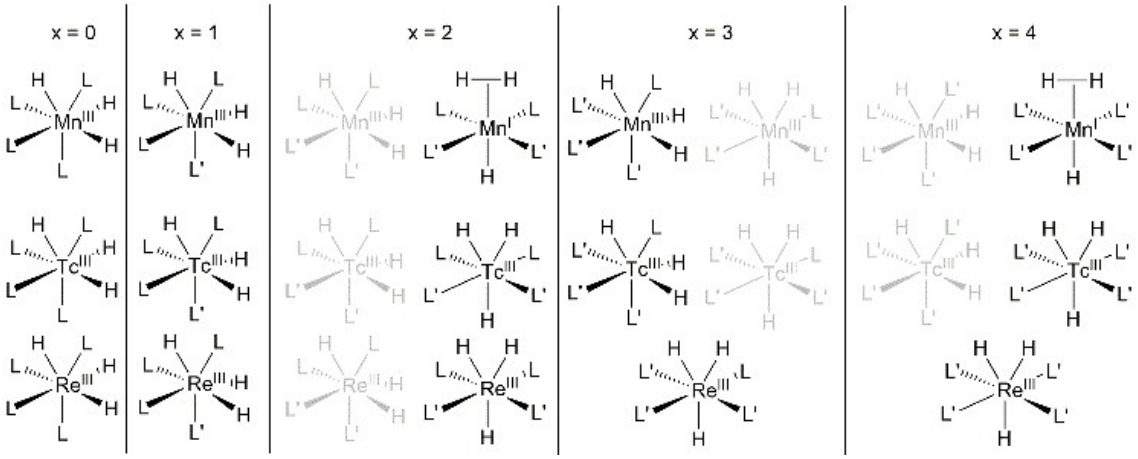

Scheme 4. Gas-phase optimized geometries of $[MH_3(L)_{4-x}(L')_x]$ complexes (M = Mn, Tc, Re; x = 0, 1, 2, 3, 4; L = PPh_3, L′ = PMe_3). Energetically less favored geometries are grey.

readily separated from the powdery mixture of side-products by a filtration over a coarse fritted glass filter.

The IR spectrum of the red-brown, crystalline product (**4a**) clearly indicates the presence of two inequivalent hydrido ligands (ν_{Re-H}: 1949 cm^{-1} and 1807 cm^{-1}). A weak absorption in-between the two asymmetric stretches might be attributed to a mixed, symmetric Re-(H,H) stretching mode (note: no H_2-character). The latter vibration is slightly blue-shifted for the ^{i}Pr (**4b**) and Ph (**4c**) derivatives and, thus, assigned to a hydride ligand *trans* to a non-phosphine ligand, while the other one is close to the vibration in rhenium hydrido complexes with the hydrido ligands in *trans* position to a PPh_3 ligand such as compounds **1**, **2** or **3**. A pattern of three bands commonly associated with a RC(H)=NR′ moiety is observed around 1600 cm^{-1}.

An X-ray diffraction study on the red-brown crystals (Figure 3) revealed the formation of a linearly-bound nitrene-type ligand. The Re–N1 bond length of 1.871(2) Å is too short for a mere single bond, while the C1–N1 bond length of 1.29(1) Å is in the range of a C–N double bond. The adjacent C1–C2 bond is a 'normal' C–C single bond with a length of 1.44(1) Å. Additionally, the Re–N1–C1 bond angle is perfectly linear, while the N1–C1–C2 bond angle is clearly bent suggesting double

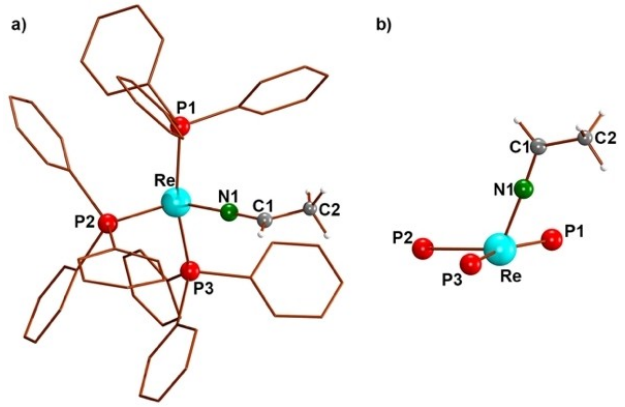

Figure 3. a) Solid state structure of $[ReH_2(NCHCH_3)(PPh_3)_3]$ (**4a**) in the solid state and b) detailed view of the azavinylidene unit. The hydrido ligands were not located. Further labels, hydrogen and carbon atoms are omitted for clarity.

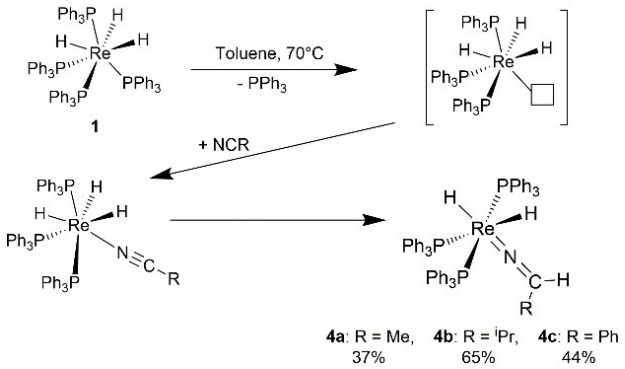

Scheme 5. Reactions of $[ReH_3(PPh_3)_4]$ (**1**) with monodentate nitriles.

bonds between Re and N1 and N1 and C1. The observed bonding features, particularly the linear Re–N–C unit,[48–60] strongly favor the assignment of compound **4a** as an azavinylidene over an interpretation as an amido complex, which would require a bent unit.[61] Recently, we observed the formation of a similar product as result of a nucleophilic attack of a fluorinated aryl lithium reagent,[62] where the obtained azavinylidene complex shows similar geometric features as discussed for **4a**.

In the present case, however, the azavinylidene is likely formed in a stepwise manner by the substitution of one PPh_3 ligand with CH_3CN, followed by a nucleophilic β-hydride migration to the polarized CN-bond (Scheme 5). As such, it resembles an isomer of the previously prepared $[ReH_3(PPh_3)_3(CH_3CN)]$.[18] Nucleophilic reactions on coordinated nitrile ligands are not unusual and in a recent report, the tendency towards such nucleophilic attacks at and β-migrations to nitrile ligands coordinated to rhenium(III) ions has been explored.[60] Either metal-bound or externally provided nucleophiles such as highly basic phosphines (e.g. PMe_3) attack the nitrile bond under formation of phosphonio–azavinylidene complexes.[60] In two recent reports, the formation of iron amido complexes from an insertion of nitriles into the Fe–H bond of iron hydrido complexes is described,[61] and a complex, stepwise mechanism for the formation of azavinylidene complexes of osmium(IV) through a migration of an hydrido ligand from osmium to a nitrile ligand has been deduced.[63] Alkyl derivatives similar to compounds **4a** or **4b** were, however, too unstable for an isolation in pure form.[63]

For a better understanding of the formation of the trihydride *versus* that of the isomeric dihydride/azavinylidene, we modelled both methyl-substituted isomers with DFT calculations. Indeed, the azavinylidene isomer **4a** is thermodynamically more favored compared with the trihydride $[ReH_3(PPh_3)_3(CH_3CN)]$ by ca. 10 kcal/mol. The previously observed stability of $[ReH_3(PPh_3)_3(CH_3CN)]$ is, thus, likely attributed to a substantial kinetic barrier between the two isomers that is readily overcome under the presented conditions starting from $[ReH_3(PPh_3)_4]$. This is similar to the situation that has been found for theoretical model complexes of osmium containing PMe_3 ligands and we, thus, believe a similar mechanism is followed for the formation of complexes **4**.[63] Related products containing hydrogen-substituted azavinylidene ligands bound to rhenium have also been obtained by electrophilic reactions, for example through protonation at coordinated nitrile carbon atoms using $(H(OEt_2)_2)(BF_4)$.[64,65] The resulting cationic rhenium species have been studied by computational methods and the azavinylidene ligands derived from protonation were suggested as three-electron donors with strong π-backbonding properties, thus resulting in stable 18-electron complexes.[64,65]

In contrast to the rhenium azavinylidenes discussed above, which are formed by protonation, a rapid decomposition of complexes **4** occurs once they are dissolved even in carefully dried solvents and in an inert atmosphere. and the formation of dark brown solutions is observed. The ^{1}H NMR spectrum of **4a** gives evidence for the presence of several species, from which $[ReH_5(PPh_3)_3]$ could be identified on the basis of its characteristic

hydrido ^{1}H NMR resonance. Similarly, a second quartet hydrido resonance is tentatively assigned to a rhenium(I) hydride with three phosphine donors similar to $[ReH(NCCH_3)(PPh_3)_3]$ based on its chemical shift of −2.8 ppm. The hydride signals of complexes **4** appear as broad resonances at ca. −4 ppm and indicate a fluxional behavior of the two hydrido ligands at room temperature. ESI+ mass spectra of such solutions show a complex superposition of signals belonging to $[ReH(NCHCH_3)(PPh_3)_3]^+$, $[ReH_2(NCHCH_3)(PPh_3)_3]^+$ and $[ReH_3(NCHCH_3)(PPh_3)_3]^+$. We, thus, also probed the feasibility of hydride abstraction from $[ReH_3(PPh_3)_4]$ with trityl hexafluorophosphate in the presence of acetonitrile. But instead of the dihydride cation $[ReH_2(NCCH_3)(PPh_3)_3]^+$, only traces of the known tetrahydride cation $[ReH_4(NCCH_3)(PPh_3)_3]^+$, which is commonly prepared by hydride abstraction from $[ReH_5(PPh_3)_3]$, were identified. Some single crystals of $[ReH_4(NCCH_3)(PPh_3)_3][PF_6]$ could be isolated from such solutions. They were of limited quality and details are described in the Supporting Information.

The three phosphine ligands in **4a** are located in one plane with the rhenium atom adopting meridional positions (Figure 3b). The *cis* angles between them are approximately 100° and the *trans* angle is 162.80(9)°. The Re–P bond lengths are around 2.36 Å to 2.37 Å. The azavinylidene ligand approaches the P–P–P plane from an angle of 116.9(3)° with respect to the central phosphorus atom and ca. 89° for the two *trans* phosphine ligands. The geometry spun by the four ligands without accounting for the hydrido ligands is closest to a distorted seesaw (SS-4, also called a divacant octahedron) as indicated by the continuous symmetry measure of 2.530.[66,67] Although the hydrido ligands could not be located in the final Fourier map, their most likely positions can be derived from an inspection of the vacancies. The largest vacancies are found below the plane spanned by the three phosphorus atoms on a mirrored N1 position and *trans* to P2. Assuming these positions, they would complete a distorted octahedral coordination sphere for the rhenium atom, which is consistent with the IR spectrum of the compound and the structure predicted by the DFT calculations. The gas-phase optimized structure of **4a** including the two hydrido ligands is shown in Figure 4. The optimized bonding parameters are in good agreement with the experimentally observed values. The gas-phase optimized Re–N bond length is 1.90 Å (exp.: 1.871(2) Å) and the C–N bond length is 1.27 Å (exp.: 1.29(1) Å). The theoretical Re–H bond lengths are Re–$H_{trans\text{-}P}$ 1.66 Å and Re–$H_{trans\text{-}N}$ 1.74 Å.

Since the previously reported azavinylidene complexes of iron, osmium, technetium and rhenium appear to be much more stable than complexes **4**,[60–65] we performed a natural bonding orbital (NBO) analysis on the electronic situation in **4a** combined with a Laplacian of the electron density $\triangle(\varrho)$ and electron localization function (ELF) mapping of the H–Re–N=C–H plane. The results are visualized in Figure 5. Surprisingly, there is no second bonding orbital between rhenium and nitrogen. Instead, the second order perturbation analysis of NBOs revealed d_{Re}-$\pi^*_{C=N}$ and p_N-σ^*_{Re-H} interactions. The π-backdonation from a rhenium d-orbital to the nitrogen-centered $\pi^*_{C=N}$ lobes is stronger than individual "π-type"

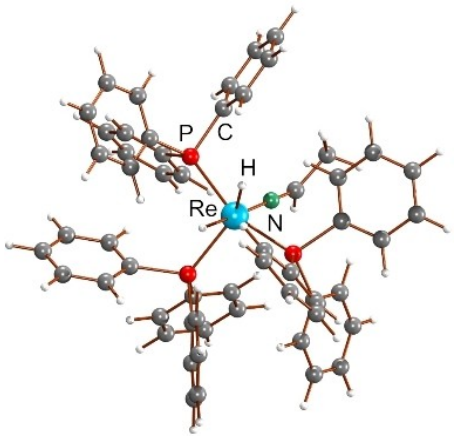

Figure 4. DFT-optimized gas-phase structure of $[ReH_2(NCHCH_3)(PPh_3)_3]$ (**4a**).

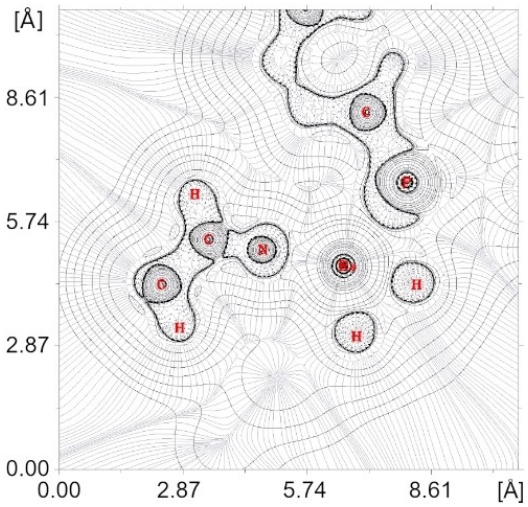

Figure 5. Laplacian mapping of the electron density $\triangle(\rho)$ in the H–Re–N=CH plane of **4a**.

delocalization from the nitrogen atoms lone-pair into either of the two σ^*_{Re-H} orbitals. Analogously, the charge localization mapping through $\triangle(\rho)$ indicates a shared electron-depletion between rhenium and the C=N bond, while charge accumulation at rhenium is pointed towards the $\pi^*_{C=N}$ lobes.

The ELF map (Figure 6) reveals a similar situation and additionally, the p-character of the additional nitrogen lone-pair becomes obvious.

Overall, the DFT calculations suggest a bonding situation of the anionic azavinylidene ligand, which is consistent with a significant π-accepting behavior of this ligand and 6 bonding valence electrons as well as one non-bonding, but constructively interacting, lone-pair at the nitrogen atom. Consequently, the bond between rhenium and nitrogen might be better described as a Re⇄N bond instead of a Re⇐N bond and therefore the instability of the complexes **4** can be understood due to the instability of the 16e$^-$ count of the distorted octahedral rhenium(III) complex, where the HOMO is the

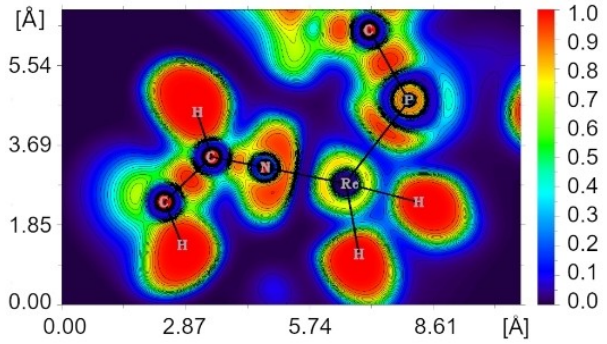

Figure 6. Electron localization function (ELF) mapping in the H–Re–N=CH plane of **4a**.

nitrogen-centered lone-pair. Further information is given as Supporting Information.

Formation of $[ReH_5(PPh_3)_3]$

$[ReH_3(PPh_3)_4]$ reacts with a variety of potential hydrogen- or 'hydride-containing' donor ligands such as thiourea, HO-$(C_6H_4(CH_3)_2)$ or pyridine. Like the reaction with PBz_3 (see above, Scheme 3), they give $[ReH_5(PPh_3)_3]$ (**5**) as the sole isolable product. From such reactions, we isolated two, previously unknown, crystalline modifications of $[ReH_5(PPh_3)_3]$ (**5**). One of them forms yellow cubes, while another polymorph consists of light green elongated plates or needles. Their IR spectra show subtle differences in the ν_{Re-H} region, but upon dissolution, their NMR spectral and mass spectrometric data are fully consistent with the published data for $[ReH_5(PPh_3)_3]$.[14,22] This behavior is consistent with that of the β and γ modifications of **5**, which were originally proposed by Ginsberg in his first preliminary report about an incomplete crystal structure determination of colorless α-$[ReH_5(PPh_3)_3]$ in 1973.[22] The α-modification was obtained from CS_2/Et_2O mixtures and crystallizes in the monoclinic space group $P2_1/n$ with cell constants of $a=$ 13.62(2) Å, $b=33.14(4)$ Å, $c=9.92(2)$ Å and $ß = 92.3(1)°$.[16] Although the submission of a future manuscript dealing with details about the β and γ modifications was announced in Ref. [22], such work was never published. The only following publication dealt with a redetermination of the crystal structure of α-$[ReH_5(PPh_3)_3]$ and was published by Cotton and Luck in 1989. The unit cell of $a=9.968(4)$ Å, $b=33.237(9)$ Å, $c=$ 13.591(4) Å and $ß = 92.27(3)°$ was equivalent to that determined by Ginsberg.[14] Additionally, the crystal structure of a co-crystal of $[ReH_5(PPh_3)_3]$ with indole and benzene was determined in 1995.[9] We therefore here report the structures of the β and γ modifications of $[ReH_5(PPh_3)_3]$ and compare the obtained bond parameters with the two previous determinations (Table 2).

The yellow modification crystallizes in the monoclinic space group $P2_1/n$ with cell constants of $a=12.8592(5)$ Å, $b=$ 16.7822(6) Å, $c=20.959(1)$ Å and $ß=91.163(4)°$ with one molecule of $[ReH_5(PPh_3)_3]$ in the asymmetric unit. The molecular structure of this compound and the coordination polyhedron of its rhenium atom are depicted in Figure 7. The green modification crystallizes in the triclinic space-group $P\bar{1}$ with cell constants of $a=10.1377(5)$ Å, $b=21.185(1)$ Å, $c=21.194(1)$ Å, $\alpha=92.542(5)°$, $ß=94.825(4)°$ and $\gamma=95.888(5)°$ with two independent molecules of $[ReH_5(PPh_3)_3]$ in the asymmetric unit. The overall arrangement of the atoms is similar in all polymorphs. Nevertheless, differences in angles up to 10° and subtle differences in bond lengths are found (Table 2).

These differences result in different continuous shape measures and therefore coordination environments with different degrees of distortion around the rhenium atoms.[42–46] Since the hydrido ligands are elusive, a comparison between the shape-measures in the different solid-state structures are only given in Table S3 in the Supporting Information. Generally, the arrangement of the ligands in all polymorphs of $[ReH_5(PPh_3)_3]$ are best described to be in-between a biaugmented trigonal prism and a triangular dodecahedron. It is apparent, that the structures in the different polymorphs are similar, but not

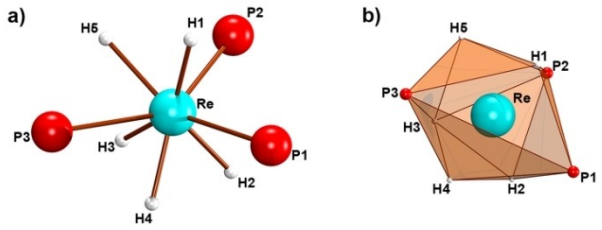

Figure 7. a) Coordination spere of the rhenium atom and b) polyhedron around Re in the solid-state structure of the yellow, monoclinic polymorph of $[ReH_5(PPh_3)_3]$ (**5**). The hydrogen atoms were located and refined freely. Further labels, hydrogen and carbon atoms are omitted for clarity.

Table 2. Comparison of Re–P bonding parameters of $[ReH_5(PPh_3)_3]$ (**5**) in all hitherto structurally characterized modifications and co-crystals. The assignment of the atoms has been adopted for all polymorphs from Figure 4. A more detailed version is given as Table S3 in the supplementary material, where additional information on the somewhat unreliable and elusive hydrido ligands and the results of the continuous symmetry measure analysis for the polyhedra around the rhenium center are given.

	$[ReH_5(PPh_3)_3]$, monoclinic, yellow	$[ReH_5(PPh_3)_3]$, triclinic, green Molecule 1	Molecule 2	$[ReH_5(PPh_3)_3]$,[14] colorless	$[ReH_5(PPh_3)_3]$·indole·benzene,[9] yellow
P1–Re1	2.3975(8)	2.407(1)	2.398(1)	2.378(2)	2.395(3)
P2–Re1	2.3896(8)	2.391(1)	2.390(1)	2.397(2)	2.387(4)
P3–Re1	2.3787(8)	2.388(1)	2.382(1)	2.403(2)	2.376(3)
P3–Re1–P2	143.27(3)	132.17(5)	104.86(4)	133.28(7)	105.6(1)
P3–Re1–P1	102.49(3)	106.23(5)	132.09(5)	107.43(7)	133.9(1)
P2–Re1–P1	108.99(3)	109.03(4)	110.03(5)	108.38(7)	110.0(1)

entirely equivalent as is supported by the corresponding P–Re–P angles. This becomes even more evident, when looking at the IR spectra of the polymorphs, which show significant differences in the complexity pattern of their Re-H valence vibrational bands. These results suggest that the frequently discussed fluxionality of the hydrido ligands in rhenium polyhydrides[1–9,11–15,18–23,68] may also play a role in the solid state.

Conclusion

The preparation of pure, crystalline $[ReH_3(PPh_3)_4]$ allows for the preparation of defined rhenium(III) polyhydrido complexes through ligand exchange procedures. A defined mono substitution of triphenylphosphine by the more basic phosphines PMe_3 and PBu_3 has been achieved for the first time. Less inert monodentate ligands such as nitriles react with $[ReH_3(PPh_3)_4]$ not only under exchange of the phosphine ligands, but they insert into one of the Re–H bonds after the phosphine exchange and give rhenium(III) azavinylidene complexes of the type $[ReH_2(PPh_3)_3(NC(H)R)]$ (R = Me, ^{i}Pr, Ph). Potential proton or hydride donors react with $[ReH_3(PPh_3)_4]$ in toluene to give the pentahydride $[ReH_5(PPh_3)_3]$. Besides the known colorless α modification, the yellow β and light green γ modifications of $[ReH_5(PPh_3)_3]$ have now been characterized. Solutions of the β and γ variants cannot be distinguished from those of α-$[ReH_5(PPh_3)_3]$. Interestingly, differences in the IR patterns and X-ray structures of the polymorphs suggest that the observed fluxionality of the five hydrido ligands in solution may be frozen to different solid-state configurations depending on the presence of different reagents.

The current report about the accessibility of novel rhenium hydrido complexes and especially the tailoring of substitution patterns with the metal in the oxidation state "+3" as well as the description of their reactivity gives some more insight into the structural chemistry of rhenium hydrides and is, thus, directly linked to the recently discussed relevance of rhenium hydrides for catalytic conversions.[4,69–71]

Experimental Section

$[ReCl_4(PPh_3)_2]$ was prepared following a literature procedure.[72] All other chemicals were reagent grade and used as received. Reactions involving oxygen- or water-sensitive compounds were performed with standard Schlenk technique. NMR spectra were recorded at 25 °C on JEOL 400 MHz ECS-400 or JNM-ECA400II spectrometers. IR spectra were recorded with an FT IR spectrometer (Nicolet iS10, Thermo Scientific). Intensities are classified as vs. = very strong, s = strong, m = medium, w = weak, vw = very weak, sh = shoulder. Electrospray ionization mass spectrometry (ESI MS) was carried out with the ESI MSD TOF unit of an Agilent 6210 TOF LC/MS system. The measurements were performed in thf, CH_2Cl_2, MeOH or mixtures of them. Elemental analyses were performed using a vario EL III CHN elemental analyzer (Elementar Analysensysteme GmbH) or a vario MICRO cube CHNS elemental analyzer. The elemental analyses for all compounds show lower carbon values than expected. This is a common observation in rhenium chemistry – especially for complexes containing additional phosphine donors – and is mostly attributed to incomplete combustion resulting from the facile formation of rhenium carbides. We nevertheless provide the best values we obtained to date from the combustion analysis. Unfortunately, spectroscopic methods are not suitable to provide an unambiguous proof for the purity of the compounds, since the majority of the products are unstable and readily release phosphines. Thus, such newly formed impurities are always detected during NMR measurements. Exemplarily, well-soluble $[ReH_5(PPh_3)_3]$ (**5**) and PPh_3 are formed upon the suspension of barely soluble $[ReH_3(PPh_3)_4]$ (**1**) in deuterated solvents and, thus, a quantitative assessment of product purity by NMR spectroscopy is prohibited. Similarly, mass spectral data is not a good descriptor for bulk purity in such samples due to similar reasons even at low ionization voltages.

Single crystal X-ray diffraction data were collected on a Bruker D8 Venture or a STOE IPDS II T. Absorption corrections were carried out by the multiscan (Bruker D8 Venture) or integration methods (STOE IPDS II T).[73,74] When the crystal quality was not feasible for data collection with Mo–Kα radiation, Cu–Kα radiation was used to enable complete data collection although absorption artifacts expectedly increased. For some compounds, the quality of the crystals did not improve even after multiple attempts of crystallization; for example many crystals of $[ReH_2(NC(H)CH_3)(PPh_3)_3]$ (**4a**) showed severe disorder and did not reveal the identity of the final non-phosphine, non-hydride ligand. Structure solutions and refinements were done with the SHELX-2008, SHELX-2014 and SHELX-2016 program packages.[75,76] The positions of the hydrido ligands have been taken from the Fourier maps and refined where possible or calculated for idealized positions. All other hydrogen atoms were calculated at idealized positions and treated with the riding model option of SHELX. The visualization of the molecular structures was done using the program DIAMOND 4.2.2.[77]

Deposition Number(s) 2197264, 2197265, 2197266, 2197267, 2197268, 2197269, 2197270, 2197271, 2197272 contain(s) the supplementary crystallographic data for this paper. These data are provided free of charge by the joint Cambridge Crystallographic Data Centre and Fachinformationszentrum Karlsruhe Access Structures service.

Computational Details. DFT calculations were performed on the high-performance computing systems of the Freie Universität Berlin ZEDAT (Curta)[78] using the program package GAUSSIAN 16.[79] The gas phase geometry optimizations were performed using coordinates derived from the X-ray crystal structures using GAUSSVIEW and Avogadro.[80,81] The calculations were performed with the hybrid density functional B3LYP.[82–84] The double-ζ pseudopotential LANL2DZ basis set with the respective effective core potential (ECP) was applied to Re in the azavinylidene calculations.[85] The double-ζ pseudopotential LANL2DZ basis set with the respective effective core potential (ECP) was applied to Re and P in the phosphine hydride calculations.[85,86] The 6-311++G** basis set was used to model all other atoms in the azavinylidene calculations.[87–91] The 6–31++G** basis set was used to model all other atoms in the pure phosphine hydride calculations.[87,89,91–94] All basis sets as well as the ECPs were obtained from the basis set exchange data base.[95–97] Frequency calculations after the optimizations confirmed the convergence of the final geometries. No negative frequencies were obtained. The entropic contribution to the free energy was corrected for low-energy modes in the azavinylidene calculations using the quasi-harmonic approximation of Grimme[98] as implemented in the freely accessible python code *GoodVibes* of Funes-Ardoiz and Paton with a cut-off at 300 cm^{-1}.[99] Further analyses were performed with the free multifunctional wavefunction analyzer *Multiwfn*.[100]

$[ReH_3(PPh_3)_4]$ (1): $[ReCl_4(PPh_3)_2]$ (580 mg, 0.67 mmol) and PPh_3 (4.5 g, 17.3 mmol) were suspended in a mixture of toluene (2 mL)

and ethanol (15 mL). The suspension was heated to ca. 90 °C and freshly ground $NaBH_4$ (400 mg, 10.6 mmol) was quickly added under vigorous stirring. An immediate gas-evolution was observed (*Caution!* H_2/borane!) and accompanied by a color change from deep red to orange-yellow. The mixture was heated for 45 min after which time the bubbling rate had decreased significantly, while no residual red particles were visible in the yellow slurry. The excess borohydride was hydrolyzed by the slow addition of water (1 mL) followed by acetone (20 mL). During these additions, the mixture was shaken vigorously to avoid clumping. The mixture was then filtered through a fine frit and washed copiously with water and acetone. Finally, it was washed with pentane and dried in air to give yellow microcrystals. Yield: 488 mg (0.39 mmol, 59%). Anal. calcd for $C_{72}H_{63}P_4Re$: C 69.8, H 5.1%; Found C 67.6, H 5.2%. IR($\tilde{\nu}$, cm^{-1}): 1973 (m, ν_{Re-H}). ESI+ MS (*m/z*): 974.2398 (calc. 974.2375) $[ReH(PPh_3)_3]^+$, 1238.3493 (calc. 1238.3445) $[M]^+$. ^1H NMR (C_6D_6, ppm): 7.98–6.71 (several m, P**Ph**$_3$), −4.65 (q, 1H, $^2J_{H,P}$ = 18.61 Hz, [Re**H**$_5$(PPh_3)$_3$]), −7.54 (3H, quint, $^2J_{H,P}$ = 40.47 Hz, [Re**H**$_3$(PPh_3)$_4$]). $^{31}P\{^1H\}$ NMR (CD_2Cl_2, ppm): 34.0 (s, [ReH_5(**P**Ph_3)$_3$]), 24.8 (s, [ReH_3(**P**Ph_3)$_4$]), −5.4 (s, **P**Ph_3).

[Re(H/D)$_3$(PPh$_3$)$_4$]: [$ReCl_4(PPh_3)_2$] (88 mg, 0.1 mmol) and PPh_3 (680 mg, 2.6 mmol) were suspended in a mixture of toluene-D_8 (1.5 mL) and MeOH–D_4 (4.5 mL). The suspension was heated to ca. 90 °C and freshly ground $NaBD_4$ (67 mg, 1.6 mmol) was quickly added under vigorous stirring. An immediate H_2 and gaseous borane evolution accompanied by a color change from deep red to orange-yellow was observed. After 10 min of heating, additional $NaBD_4$ (10 mg, 0.2 mmol) was added and the heating was continued until the bubbling ceased (ca. 10 min). The excess of borodeuteride was hydrolyzed by the slow addition of D_2O (0.5 mL) followed by acetone (ca. 20 mL) under vigorous stirring. After cooling to RT, the mixture was filtered through a fine frit and washed copiously with water and acetone. Finally, it was washed with diethyl ether and pentane before drying in air to give yellow microcrystals. Yield: 46 mg (0.04 mmol, 37%). IR(KBr, $\tilde{\nu}$, cm^{-1}): 1973 (m, ν_{Re-H}), 1715 (m, ν_{Re-D}).

[ReH$_3$(PPh$_3$)$_3$(PMe$_3$)] (2): [$ReH_3(PPh_3)_4$] (124 mg, 0.1 mmol) was suspended in dry, degassed toluene (1 mL) under Ar. A solution of PMe_3 in THF (0.6 mL, 0.6 mmol) was added. The resulting yellow suspension was heated to ca. 70 °C (over ca. 30 min) at which point the suspension became a clear yellow solution. Methanol (15 mL) was immediately added after the complete dissolution to the still hot solution and the mixture was stored in a refrigerator for 3 h. The formed, bright yellow crystals were filtered off, washed with MeOH and hexane and quickly dried in vacuum (*Caution!* The product is not very stable in vacuum!). The compound has only a limited stability as a solid and slowly decomposes over several weeks of storage at room temperature. Storage in a freezer is recommended. Yield: 60 mg (0.06 mmol, 57%). Anal. calcd for $C_{57}H_{57}P_4Re$: C 65.1, H 5.5%; Found C 61.6, H 5.2%. IR ($\tilde{\nu}$, cm^{-1}): 1947 (m, ν_{Re-H}), 1900 (m, ν_{Re-H}). ESI+ MS (*m/z*): 1053.3109 (calc. 1053.3052) $[M+H]^+$. ^1H NMR (C_6D_6, ppm): 7.72–7.37 (m, 19H, P**Ph**$_3$), 7.04–6.80 (m, 29H, P**Ph**$_3$), 1.13 (d, $^2J_{H,P}$ = 7.17 Hz, P**Me**$_3$), −7.41 (3H, dq, $^2J_{H,P}$ = 33.72 Hz, $^2J_{H,P}$ = 30.44 Hz, [Re**H**$_3$(PPh_3)$_3$(PMe_3)]). $^{31}P\{^1H\}$ NMR (CD_2Cl_2, ppm): 34.0 (d, $^2J_{P,P}$ = 16.6 Hz, [ReH_3(**P**Ph_3)$_3$(PMe_3)]), −5.4 (s, **P**Ph_3), −53.8 (q, $^2J_{P,P}$ = 16.8 Hz, [$ReH_3(PPh_3)_3$(**P**Me_3)]).

[ReH$_3$(PPh$_3$)$_3$(PBu$_3$)] (3): [$ReH_3(PPh_3)_4$] (155 mg, 0.13 mmol) was suspended in dry, degassed toluene (6 mL) under Ar. Neat PBu_3 (0.185 mL, 0.75 mmol) was added. The resulting yellow suspension was heated to ca. 70 °C and the temperature kept for 1 min at which point the suspension became a clear yellow solution. Methanol (27 mL) was immediately layered after the complete dissolution onto the still hot solution. The methanol was slowly shaken into the toluene and once initial crystallization began, the mixture was stored in the refrigerator for 3 h followed by storage for 1 week in the freezer. The thus formed bright yellow crystals were filtered off, washed with MeOH and hexane. A final washing was performed with a small quantity of diethyl ether. Since the product is soluble in this solvent, the washing should be done with a minimum amount and quickly. The crystals were suitable for X-ray diffraction, but slowly decomposed at room temperature, which could be identified by a gradual appearance of the smell of PBu_3. Yield: 64 mg (0.05 mmol, 42%). Anal. calcd for $C_{66}H_{75}P_4Re$: C 67.3, H 6.4%; Found C 58.8, H 5.6%. IR ($\tilde{\nu}$, cm^{-1}): 1943 (m, ν_{Re-H}), 1909 (m, ν_{Re-H}), 1817 (w, ν_{Re-H}). ESI+ MS (*m/z*): 914.3300 (calc. 914.3313) $[ReH(PPh_3)_2(PBu_3)]^+$, 1178.4348 (calc. 1178.4383) $[M]^+$. ^1H NMR (C_6D_6, ppm): 7.61–7.42 (m, 17H, P**Ph**$_3$), 7.01–6.84 (m, 28H, P**Ph**$_3$), 1.53–1.41 (m, 6H, P(C**H**$_2$CH$_2$CH$_2$CH$_3$)$_3$), 1.41–1.30 (m, 6H, P-(CH$_2$C**H**$_2$CH$_2$CH$_3$)$_3$), 1.10 (h, 6H, $^3J_{H,H}$ = 7.21 Hz, P(CH$_2$CH$_2$C**H**$_2$CH$_3$)$_3$), 1.10 (t, 9H, $^3J_{H,H}$ = 7.21 Hz, P(CH$_2$CH$_2$CH$_2$C**H**$_3$)$_3$), −4.65 (0H, q, $^2J_{H,P}$ = 18.64 Hz, [Re**H**$_5$(PPh_3)$_3$), −5.64 (0H, q, $^2J_{H,P}$ = 18.88 Hz, [Re**H**$_5$(PPh_3)$_2$(PBu_3)]), −7.38 (3H, dq, $^2J_{H,P}$ = 36.10 Hz, $^2J_{H,P}$ = 31.71 Hz, [Re**H**$_3$(PPh_3)$_3$(PBu_3)]). $^{31}P\{^1H\}$ NMR (CD_2Cl_2, ppm): 37.5 (s, [ReH_5(**P**Ph_3)$_2$(PBu_3)]), 33.8 (s, [ReH_5(**P**Ph_3)$_3$]), 30.4 (d, $^2J_{P,P}$ = 18.2 Hz, [ReH_3(**P**Ph_3)$_3$(PBu_3)]), 0.3 (s, [$ReH_5(PPh_3)_2$(**P**Bu_3)]), −5.4 (s, **P**Ph_3), −20.3 (q, $^2J_{P,P}$ = 18.3 Hz, [$ReH_3(PPh_3)_3$(**P**Bu_3)]).

[ReH$_2$(NC(H)CH$_3$)(PPh$_3$)$_3$] (4a): [$ReH_3(PPh_3)_4$] (63 mg, 0.05 mmol) was suspended in dry, degassed toluene (1 mL) under Ar. Dry, degassed CH_3CN (1 drop) was added. The resulting yellow suspension was heated to ca. 70 °C and the temperature kept until the suspension became a clear orange red solution. Acetone (1 mL) and methanol (7 mL) were added to the cooled solution. Yellow microcrystals of [$ReH_3(PPh_3)_3(NCCH_3)$], [$ReH_5(PPh_3)_3$] and red microcrystals of [$ReH_2(NCHCH_3)(PPh_3)_3$] precipitated. The mixture was stored in the refrigerator overnight, after which time large red-brown crystals formed among the orange microcrystalline precipitate. The large red crystals were separated from the precipitate by filtration through a coarse (P2) fritted glass filter. They were washed with MeOH and hexane before drying in vacuum. The crystals were suitable for X-ray diffraction. Yield: 19 mg (0.02 mmol, 37%). Anal. calcd for $C_{56}H_{51}NP_3Re$: N 1.4, C 66.1, H 5.1%; Found N 1.4, C 62.5, H 4.8%. IR($\tilde{\nu}$, cm^{-1}): 1949 (m, ν_{Re-H}), 1807 (m, ν_{Re-H}). ESI+ MS (*m/z*): 1016.2754 (calc. 1016.2719) [M–H]$^+$, 1017.2780 (calc. 1017.2797) $[M]^+$, 1018.2837 (calc. 1018.2875) $[M+H]^+$, 1034.2828 (calc. 1034.2824) $[M+H+O_{PPh3}]^+$, 1088.3255 (calc. 1088.3295) $[M+thf]^+$, 1104.3410 (calc. 1104.3244) $[M+thf+O_{PPh3}]^+$, 1120.3341 (calc. 1120.3244) $[M+thf+2O_{PPh3}]^+$, 1136.3150 (calc. 1136.3142) $[M+thf+3O_{PPh3}]^+$. ^1H NMR (C_6D_6, ppm): −2.85 (q, $^2J_{H,P}$ = 50.40 Hz, tentatively: [Re**H**(PPh_3)$_3$($NCCH_3$)]), −4.00 (s broad, FWHM = 185 Hz, [Re**H**$_2$(NC(H)CH_3) (PPh_3)$_3$]), −4.65 (0H, q, $^2J_{H,P}$ = 17.55 Hz, [Re**H**$_5$(PPh_3)$_3$]).

[ReH$_2$(NC(H)^{i}Pr)(PPh$_3$)$_3$] (4b): [$ReH_3(PPh_3)_4$] (63 mg, 0.05 mmol) was suspended in dry, degassed toluene (1 mL) under Ar. Dry, degassed ^{i}PrCN (1 drop) was added. The resulting yellow suspension was heated to ca. 70 °C and the temperature kept until the suspension became a clear orange red solution. Methanol (7 mL) was added to the cooled solution. Orange microcrystals precipitated. The mixture was stored in the refrigerator overnight, after which time more orange microcrystalline precipitate occurred. The orange yellow powder was filtered off, washed with MeOH and hexane and dried in vacuum. Yield: 34 mg (0.03 mmol, 65%). Anal. calcd for $C_{58}H_{55}NP_3Re$: N 1.3, C 66.7, H 5.3; Found N 1.4, C 64.1, H 5.7%. IR(KBr, $\tilde{\nu}$, cm^{-1}): 1969 (m, ν_{Re-H}), 1784 (m, ν_{Re-H}). ESI+ MS (*m/z*): 768.2021 (calc. 768.1962) [M–PPh_3–H_2–H]$^+$, 809.2289 (calc. 809.1753) [M–PPh_3–H+K]$^+$, 1030.2972 (calc. 1030.2875) [M–H_2–H]$^+$, 1071.3215 (calc. 1071.2667) [M–H+K]$^+$. ^1H NMR (CD_2Cl_2, ppm): −4.39 (s broad, FWHM = 169 Hz, [Re**H**$_2$(NC(H)^{i}Pr) (PPh_3)$_3$]), −5.33 (q, $^2J_{H,P}$ = 16.74 Hz, [Re**H**$_5$(PPh_3)$_3$]), −7.95 (quint, $^2J_{H,P}$ = 37.41 Hz, [Re**H**$_3$(PPh_3)$_4$]).

[$ReH_2(NC(H)Ph)(PPh_3)_3$] (4c): [$ReH_3(PPh_3)_4$] (124 mg, 0.1 mmol) was suspended in dry, degassed toluene (2 mL) under Ar. Dry, degassed PhCN (2 drops) was added. The color changed to orange-red immediately. The resulting suspension was heated up to ca. 70 °C resulting in a blood red clear solution. Methanol (24 mL) was added to the cooled solution and orange red microcrystals precipitated. The mixture was stored in the refrigerator overnight, after which time more orange red microcrystalline precipitate occurred. The precipitate was filtered off, washed with MeOH and dissolved in Et_2O leaving a red residue. Addition of the Et_2O solution to methanol and evaporation of the ether at RT over 3 h resulted in the formation of red microcrystals. They were filtered off, washed with MeOH and dried in vacuum. Yield: 47 mg (0.04 mmol, 44%). Anal. calcd for $C_{61}H_{53}NP_3Re$: N 1.3, C 67.9, H 5.0%; Found N: 1.4, C 65.0, H 5.6%. IR($\tilde{\nu}$, cm^{-1}): 1967 (m, ν_{Re-H}), 1811 (m, ν_{Re-H}). ESI+ MS (m/z): 937.2673 (calc. 937.2170) $[Re(PPh_3)_2(P(C_6H_5)_2)(NCCH_3)]^+$, 973.2344 (calc. 973.2296) $[M–H_2–NCHPh]^+$, 1077.2882 (calc. 1077.2798) $[M–H_2]^+$, 1079.2967 (calc. 1079.2954) $[M]^+$. ^1H NMR (CD_2Cl_2, ppm): −4.35 (s broad, FWHM = 141 Hz, [Re**H_2**(NC(H)Ph)$(PPh_3)_3$]), −5.29 (q, [Re**H_5**$(PPh_3)_3$]), −6.33 (s broad, FWHM = 109 Hz, tentatively: [Re**H_3**$(PPh_3)_3$(NCPh)]).

Acknowledgements

We gratefully acknowledge the assistance of the Core Facility BioSupraMol supported by the DFG and High-Performance-Computing (HPC) Centre of the Zentraleinrichtung für Datenverarbeitung (ZEDAT) of the Freie Universität Berlin for computational time and support. We thank Dr. Peter Müller (MIT) for the help with the refinement of the severe disorder in the hexagonal polymorph of [$ReH_3(PPh_3)_4$] (**1**). Open Access funding enabled and organized by Projekt DEAL.

Conflict of Interest

The authors declare no conflict of interest.

Data Availability Statement

The data that support the findings of this study are included in the Supporting Information. Further data e.g. coordinates of DFT optimized structures available from the corresponding author upon reasonable request.

Keywords: azavinylidene · hydrides · phosphines · rhenium

[1] Y. Tao, W. Zou, G.-G. Luo, E. Kraka, *Inorg. Chem.* **2021**, *60*, 2492–2502.
[2] A. G. Scorzelli, B. E. Macalush, D. V. Naik, G. A. Moehring, *Inorg. Chim. Acta* **2021**, *516*, 120120.
[3] A. C. Castro, D. Balcells, M. Repisky, T. Helgaker, M. Cascella, *Inorg. Chem.* **2020**, *59*, 17509–17518.
[4] L. J. Donnelly, S. Parsons, C. A. Morrison, S. P. Thomas, J. B. Love, *Chem. Sci.* **2020**, *11*, 9994–9999.
[5] D. J. Streisel, A. L. Petrou, A. G. Scorzelli, B. E. Macalush, H. M. Siebert, G. S. Torres, C. M. Joswick, G. A. Moehring, *Inorg. Chim. Acta* **2019**, *496*, 119028.
[6] H. Jin, Z. Zhu, N. Jin, J. Xie, Y. Cheng, C. Thu, *Org. Chem. Front.* **2015**, *2*, 378–382.
[7] J. C. Lee Jr., W. Yao, R. H. Crabtree, H. Rüegger, *Inorg. Chem.* **1996**, *35*, 695–699.
[8] S. Fontán, A. Marchi, L. Marvelli, R. Rossi, S. Antoniutti, G. Albertin, *J. Chem. Soc. Dalton Trans.* **1996**, *13*, 2779–2785.
[9] J. Wessel, C. L. Lee Jr., E. Peris, G. P. A. Yap, J. B. Fortin, J. S. Ricci, G. Sini, A. Albinati, T. F. Koetzle, O. Eisenstein, A. L. Rheingold, R. H. Crabtree, *Angew. Chem. Int. Ed. Engl.* **1995**, *34*, 2507–2509.
[10] J. R. Dilworth, J. Hu, J. R. Miller, D. L. Hughes, J. A. Zubieta, Q. Chen, *J. Chem. Soc. Dalton Trans.* **1995**, *1*, 3153–3164.
[11] X.-L. Luo, J. A. K. Howard, R. H. Crabtree, *Magn. Reson. Chem.* **1991**, *29*, 589–593.
[12] F. A. Cotton, R. L. Luck, *Inorg. Chem.* **1989**, *28*, 2181–2186.
[13] D. M. Lunder, M. A. Green, W. E. Streib, K. G. Caulton, *Inorg. Chem.* **1989**, *28*, 4527–4531.
[14] F. A. Cotton, R. L. Luck, *J. Am. Chem. Soc.* **1989**, *111*, 5757–5761.
[15] D. G. Hamilton, R. H. Crabtree, *J. Am. Chem. Soc.* **1988**, *110*, 4126–4133.
[16] G. J. Kubas, *Acc. Chem. Res.* **1988**, *21*, 120–128.
[17] G. A. Moehring, R. A. Walton, *Inorg. Chem.* **1987**, *26*, 2910–2912.
[18] G. A. Moehring, R. A. Walton, *J. Chem. Soc. Dalton Trans.* **1987**, *4*, 715–720.
[19] J. D. Allison, G. A. Moehring, R. A. Walton, *J. Chem. Soc. Dalton Trans.* **1986**, *1*, 67–72.
[20] G. G. Hlatky, R. H. Crabtree, *Coord. Chem. Rev.* **1985**, *65*, 1–48.
[21] W. A. Kupiński, J. C. Huffman, J. W. Bruno, K. G. Caulton, *J. Am. Chem. Soc.* **1984**, *106*, 8128–8136.
[22] A. P. Ginsberg, S. C. Abrahams, P. B. Jamieson, *J. Am. Chem. Soc.* **1973**, *95*, 4751–4752.
[23] J. Chatt, R. S. Coffey, *J. Chem. Soc. A* **1969**, *0*, 1963–1972.
[24] M. Freni, R. Demichelis, D. Giusto, *J. Inorg. Nucl. Chem.* **1967**, *29*, 1433–1439.
[25] M. Freni, V. Valenti, *Gazz. Chim. Ital.* **1961**, *91*, 1357–1363.
[26] L. Malatesta, *Final Report*, *New Hydrides of Transition Metals*, **1963**. Unclassified AD 434555; Defense Documentation Center for Scientific and Technical Information; Cameron Station, Alexandria, Virginia.
[27] M. Freni, P. Romiti, *Inorg. Nucl. Chem. Lett.* **1970**, *6*, 167–170.
[28] M. R. Espinosa, M. C. Ertem, M. Barakat, Q. J. Bruch, A. P. Deziel, M. R. Elsby, F. Hasanayn, N. Hazari, A. J. M. Miller, M. V. Pecoraro, A. M. Smith, N. E. Smith, *J. Am. Chem. Soc.* **2022**,*144*, 17939–19954.
[29] W. D. Jones, J. A. Maguire, *Organometallics* **1987**, *6*, 1728–1737.
[30] J. Chatt, R. S. Coffey, *J. Chem. Soc. (A) Inorg. Phys. Theor.* **1969**, *86*, 1963–1972.
[31] M. R. Jungfer, L. Elsholz, U. Abram, *Organometallics* **2021**, *40*, 3095–3112.
[32] M. Freni, V. Valenti, *J. Inorg. Nucl. Chem.* **1961**, *16*, 240–245.
[33] J. Chatt, G. A. Rowe, *J. Chem. Soc.* **1962**, 4019–1433.
[34] J. Chatt, J. D. Garforth, N. P. Johnson, G. A. Rowe, *J. Chem. Soc.* **1964**, 1012–1020.
[35] J. Chatt, C. D. Falk, G. J. Leigh, R. J. Paske, *J. Chem. Soc. A* **1969**, *9*, 2288–2293.
[36] X. Schoultz, T. I. A. Gerber, R. Betz, *Inorg. Chem. Commun.* **2016**, *69*, 45–46.
[37] D. M. Heinekey, W. J. Oldham Jr., *Chem. Rev.* **1993**, *93*, 913–926.
[38] D. A. Roberts, G. L. Geoffroy, *J. Organomet. Chem.* **1981**, *214*, 221–231.
[39] L. Helm, *Coord. Chem. Rev.* **2008**, *252*, 2346–2361.
[40] R. G. Teller, R. Bau, Crystallographic studies of transition metal hydride complexes. In: *Metal Complexes. Structure and Bonding*, *Vol. 44*, **1981**, Springer, Berlin, Heidelberg.
[41] R. Bau, M. H. Drabnis, *Inorg. Chim. Acta* **1997**, *259*, 27–50.
[42] M. Llunell, D. Casanova, J. Cirera, P. Alemany, S. Alvarez, S. *SHAPE Program for the Stereochemical Analysis of Molecular Fragments by Means of Continuous Shape Measures and Associated Tools.* **2013**, version 2.1., http://www.ee.ub.edu/index.php?option=com_jdownloads&Itemid=529&view=viewcategory&catid=4.
[43] M. Pinsky, D. Avnir, *Inorg. Chem.* **1998**, *37*, 5575–5582.
[44] D. Casanova, J. Cirera, M. Llunell, P. Alemany, D. Avnir, S. Alvarez, *J. Am. Chem. Soc.* **2004**, *126*, 1755–1763.
[45] J. Cirera, E. Ruiz, S. Alvarez, *Chem. Eur. J.* **2006**, *12*, 3162–3167.
[46] D. Casanova, P. Alemany, J. M. Bofill, S. Alvarez, *Chem. Eur. J.* **2003**, *9*, 1281–1295.
[47] J. D. Allison, T. E. Wood, R. E. Wild, R. A. Walton, *Inorg. Chem.* **1982**, *21*, 3540–3546.
[48] V. Y. Kukushkin, A. J. L. Pombeiro, *Inorg. Chim. Acta* **2005**, *358*, 1–21.
[49] A. J. L. Pombeiro, V. Y. Kukushkin, Reactivity of Coordinated Nitriles. In *Comprehensive Coordination Chemistry II*; McCleverty, J. A., Meyer, T. J., Eds.; Pergamon: Oxford, **2003**; pp 639–660.

[50] V. Y. Kukushkin, A. J. L. Pombeiro, *Chem. Rev.* **2002**, *102*, 1771–1802.
[51] R. A. Michelin, M. Mozzon, R. Bertani, *Coord. Chem. Rev.* **1996**, *147*, 299–338.
[52] C. P. Chin, Y. Ren, J. Berry, S. A. Knott, C. C. McLauchlan, L. F. Szczepura, *Dalton Trans.* **2018**, *47*, 4653–4660.
[53] A. J. Osinski, D. L. Morris, R. S. Herrick, C. J. Ziegler, *Inorg. Chem.* **2017**, *56*, 14734–14737.
[54] W. C. Corbin, G. S. Nichol, Z. Zheng, *Inorg. Chem.* **2016**, *55*, 9505–9508.
[55] P. Gómez-Iglesias, J. M. Martín-Alvarez, D. Miguel, F. Villafañe, *Dalton Trans.* **2015**, *44*, 17478–17481.
[56] P. Gomez-Iglesias, F. Guyon, A. Khatyr, G. Ulrich, M. Knorr, J. M. Martin-Alvarez, D. Miguel, F Villafane, *Dalton Trans.* **2015**, *44*, 17516–17528.
[57] V. Yempally, W. Y. Fan, B. A. Arndtsen, A. A. Bengali, *Inorg. Chem.* **2015**, *54*, 11441–11449.
[58] P. Gómez-Iglesias, M. Arroyo, S. Bajo, C. Strohmann, D. Miguel, F. Villafañe, *Inorg. Chem.* **2014**, *53*, 12437–12448.
[59] M. E. Viguri, M. A. Huertos, J. Perez, L. Riera, *Chem. Eur. J.* **2013**, *19*, 12974–12977.
[60] K.-F. Lee, T. Yang, L.-Y. Tsang, H. H. Y. Sung, I. D. Williams, L. Lin, G. Jia, *Organometallics* **2021**, *40*, 358–369.
[61] Y. Yu, A. R. Sadique, J. M. Smith, T. R. Dugan, E. C. Cowley, W. W. Brennessel, C. J. Flaschenriem, E. Bill, T. R. Cundari, P. L. Holland, *J. Am. Chem. Soc.* **2008**, *130*, 6624–6638.
[62] M. J. Ernst, M. R. Jungfer, U. Abram, *Organometallics* **2022**, *41*, 1216–1224.
[63] J. C. Babón, M. A. Esteruelas, I. Fernández, A. M. López, E. Oñate, *Inorg. Chem.* **2019**, *58*, 8673–8684.
[64] M. F. G. da Silva, J. J. R. F. da Silva, A. J. L. Pombeiro, *Inorg. Chem.* **2002**, *41*, 219–228.
[65] M. L. Kuznetsov, A. A. Nazarov, A. J. L. Pombeiro, *J. Phys. Chem. A* **2005**, *109*, 8187–8198.
[66] J. Cirera, P. Alemany, S. Alvarez, *Chem. Eur. J.* **2004**, *10*, 190–207.
[67] S. Alvarez, D. Avnir, M. Llunell, M. Pinsky, *New J. Chem.* **2002**, *26*, 996–1009.
[68] D. V. Naik, G. A. Moehring, *Molecules* **2022**, *27*, 5017.
[69] J. C. Babón, M. A. Esteruelas, A. M. López, *Chem. Soc. Rev.* **2022**, *51*, 9717–9758.
[70] M. L. Gothe, K. L. C. Silva, A. L. Figueredo, J. L. Fiorio, J. Rozendo, B. Manduca, V. Simizu, R. S. Freire, M. A. S. Garcia, P. Vidinha, *Eur. J. Inorg. Chem.* **2021**, *39*, 4043–4065.
[71] L. J. Donnelly, T. Faber, C. A. Morrison, G. S. Nichol, S. P. Thomas, J. B. Love, *ACS Catal.* **2021**, *11*, 7394–7400.
[72] G. Rouschias, G. Wilkinson, *J. Chem. Soc. A* **1967**, *6*, 993–1000.
[73] G. M. Sheldrick, *SADABS*, University of Göttingen, Germany, **1996**.
[74] P. Coppens, The Evaluation of Absorption and Extinction in Single-Crystal Structure Analysis. Crystallographic Computing, Copenhagen, Muksgaard, **1979**.
[75] G. M. Sheldrick, *Acta Crystallogr. Sect. S* **2008**, *64*, 112–122.
[76] G. M. Sheldrick, *Acta Crystallogr. Sect. C* **2015**, *71*, 3–8.
[77] *Diamond – Crystal and Molecular Structure Visualization*, Crystal Impact – Dr. H. Putz & Dr. K. Brandenburg GbR, Bonn, Germany.
[78] High performance computing (HPC) system Curta at Freie Universität Berlin. DOI: 10.17169/refubium-26754.
[79] M. J. Frisch, G. W. Trucks, H. B. Schlegel, G. E. Scuseria, M. A. Robb, J. R. Cheeseman, G. Scalmani, V. Barone, G. A. Petersson, H. Nakatsuji, X. Li, M. Caricato, A. V. Marenich, J. Bloino, B. G. Janesko, R. Gomperts, B. Mennucci, H. P. Hratchian, J. V. Ortiz, A. F. Izmaylov, J. L. Sonnenberg, D. Williams-Young, F. Ding, F. Lipparini, F. Egidi, J, Goings, B. Peng, A. Petrone, T. Henderson, D. Ranasinghe, V. G. Zakrzewski, J. Gao, N. Rega, G. Zheng, W. Liang, M. Hada, M. Ehara, K. Toyota, R. Fukuda, J. Hasegawa, M. Ishida, T. Nakajima, Y. Honda, O. Kitao, H. Nakai, T. Vreven, K. Throssell, J. A. Montgomery Jr., J. E. Peralta, F. Ogliaro, M. J. Bearpark, J. J. Heyd, E. N. Brothers, K. N. Kudin, V. N. Staroverov, T. A. Keith, R. Kobayashi, J. Normand, K. Raghavachari, A. P. Rendell, J. C. Burant, S. S. Iyengar, J. Tomasi, M. Cossi, J. M. Millam, M. Klene, C. Adamo, R. Cammi, J. W. Ochterski, R. L. Martin, K. Morokuma, O. Farkas, J. B. Foresman, D. J. Fox, Gaussian 16, Revision B.01, Gaussian, Inc., Wallingford CT, **2016**.
[80] R. Dennington, T. A. Keith, J. M. Millam, GaussView, Version 6, Semichem Inc., Shawnee Mission, KS, **2016**.
[81] M. D. Hanwell, D. E. Curtis, D. C. Lonie, C. Vandermeersch, E. Zurek, G. R. Hutchison, *J. Cheminf.* **2012**, *4*:17.
[82] S. H. Vosko, L. Wilk, M. Nusair, *Can. J. Phys.* **1980**, *58*, 1200–1211.
[83] A. D. Becke, *J. Chem. Phys.* **1993**, *98*, 5648–5652.
[84] C. Lee, W. Yang, R. G. Parr, *Phys. Rev.* **1988**, *B37*, 785–789.
[85] P. J. Hay, W. R. Wadt, *J. Chem. Phys.* **1985**, *82*, 299–310.
[86] W. R. Wadt, P. J. Hay, *J. Chem. Phys.* **1985**, *82*, 284–298.
[87] M. M. Francl, W. J. Pietro, W. J. Hehre, J. S. Binkley, M. S. Gordon, D. J. DeFrees, J. A. Pople, *J. Chem. Phys.* **1982**, *77*, 3654–3665.
[88] A. D. McLean, G. S. Chandler, *J. Chem. Phys.* **1980**, *72*, 5639–5648.
[89] G. W. Spitznagel, T. Clark, P. V. R. Schleyer, W. J. Hehre, *J. Comput. Chem.* **1987**, *8*, 1109–1116.
[90] R. Krishnan, J. S. Binkley, R. Seeger, J. A. Pople, *J. Chem. Phys.* **1980**, *72*, 650–654.
[91] T. Clark, J. Chandrasekhar, G. W. Spitznagel, P. V. R. Schleyer, *J. Comput. Chem.* **1983**, *4*, 294–301.
[92] R. Ditchfield, W. J. Hehre, J. A. Pople, *J. Chem. Phys.* **1971**, *54*, 724–728.
[93] P. C. Hariharan, J. A. Pople, *Theor. Chim. Acta* **1973**, *28*, 213–222.
[94] W. J. Hehre, R. Ditchfield, J. A. Pople, *J. Chem. Phys.* **1972**, *56*, 2257–2261.
[95] B. P. Pritchard, D. Altarawy, B. Didier, T. D. Gibsom, T. L. Windus, *J. Chem. Inf. Model.* **2019**, *59*, 4814–4820.
[96] K. L. Schuchardt, B. T. Didier, T. Elsethagen, L. Sun, V. Gurumoorthi, J. Chase, J. Li, T. L. Windus, *J. Chem. Inf. Model.* **2007**, *47*, 1045–1052.
[97] D. Feller, *J. Comput. Chem.* **1996**, *17*, 1571–1586.
[98] S. Grimme, *Chem. Eur. J.* **2012**, *18*, 9955–9964.
[99] R. Paton, I. Funes-Ardoiz, https://zenodo.org/badge/latestdoi/16266/bobbypaton/GoodVibes.
[100] T. Lu, F. Chen, *J. Comput. Chem.* **2012**, *33*, 580–592.

Manuscript received: October 25, 2022
Accepted manuscript online: January 11, 2023
Version of record online: March 6, 2023